Bulletin of Natural Sciences Research
Vol. 15, No. 1, 2025.
DOI: https://doi.org/10.5937/bnsr15-57655
Original Scientific Paper

AN IMPROVED CANOPY INTERCEPTION SCHEME INTO BIOGEOCHEMICAL ANALYSIS OF WATER FLUXES IN SUBALPINE CONIFEROUS FOREST (NORTHERN ITALY)

POLINA LEMENKOVA[1*]

[1]Alma Mater Studiorum – University of Bologna, Department of Biological, Geological and Environmental Sciences, Via Irnerio 42, IT-40126 Bologna, Emilia-Romagna, Italy

ABSTRACT

The delicate ecosystems of the Alps' subalpine forests are crucial to water supplies as well as the local and mesoscale climate regulators. Although earlier research has assessed various aspects of the water balance, there is currently a dearth of studies that directly measure every component of the water budget. Furthermore, little is understood about the frequency and impact of fog as well as how forest layout affects water balance. Using the eddy covariance technique, sap flow sensors, phenocam images, throughfall and stemflow gauges, soil moisture sensors, water discharge measurements, and a fog interception gauge, we carried out a thorough investigation of a subalpine coniferous forest at the Renon site in the Italian Alps. Furthermore, we measured the leaf area and lichen occurrence as possible canopy water storage components. Large amount of precipitation was reflected by the canopy interception in spruce and coniferous forest. Although fog alone had no effect on total water intake, it did result in a tiny but noticeable increase in throughfall during mixed fog and rain precipitation events, however this effect seemed to be less significant than in cloud forests that are tropical or subtropical. At the catchment level, the annual balance (November–October) was almost perfectly closed when all input and output components were taken into account. This paper contributes to the ecological monitoring of the Alpine forests in South Tyrol, Northern Italy.

Keywords: Fog, Canopy Interception, Evaporation, Throughfall, Forest, Rainfall, Northern Italy.

INTRODUCTION

Forests are valuable resources in natural systems with high value in ecological, economic, social, and aesthetic services. This includes habitats for biodiversity, the supply of food, medicine, and auxiliary products, recreational opportunities, and aesthetic qualities. Important service of forest for ecosystems consists in the control of the hydrologic cycle and the preservation of soil resources. Forests affect local climate settings by exchanging carbon dioxide, water, and energy, with the atmosphere.

In view of the important link between forests and climate, it is crucial to evaluate the processes of water cycle within forest ecosystems. The statistical models and numerical parameterizations of the climate parameters and Earth's land surface responses provide us with information of how forests contributes to the regulation of local climate through measuring water balance. In hydrological techniques, measurements of the water balance components in forests are typically surrounded by widely accepted oversimplifications and significant uncertainties (Minić, 2001; Ristić Vakanjac et al., 2015; Lemenkova, 2024a). The latter is addressed in ecohydrology by dividing evapotranspiration into transpiration by the vegetation and evaporation from forest interior surfaces (Lemenkova, 2022a; Ahmed et al., 2025; Crișu et al., 2025). Evaporation from canopy interception in forests can currently only be determined indirectly or modeled, even though sapflow sensors and canopy chambers, for example, can detect soil evaporation and tree transpiration directly.

Nevertheless, there are still difficulties to model the correlation between key environmental factors. Aerodynamic modeling of energy exchange was employed in the early attempts to land surface parameterizations. Nevertheless, in these models, the effects of forests vegetation were not explicitly computed neither evaluated. In such models heat flow was controlled by the availability of soil water, and the hydrologic cycle was reduced to a soil water model. Using the traditional Penman-Monteith-equation by a factor of two or more, or the rate of wet canopy evaporation estimated from eddy covariance data (Zhu et al., 2024; Kang et al., 2025) or as the variations between precipitation, throughfall, and stemflow. Existing methods use spatial analysis (Klaučo et al., 2013; Lemenkova, 2024b), statistical techniques for remote sensing data processing (Roljević et al., 2012; Lemenkova, 2021a; Zhang et al., 2025), or hydrogeological and applied engineering approaches to data modelling (Lindh and Lemenkova, 2023; Can et al., 2025; Shaddad et al., 2025).

Forecasting dynamics of climate variables has also become an important aspect of environmental management, as it allows for proactive intervention strategies (Lemenkova, 2021b; 2023a; Cai & Shi, 2025; Ji et al., 2025). Example of an ecological influence on climate in forest ecosystems is

* Corresponding author: polina.lemenkova2@unibo.it

demonstrated by paired climate simulations, which control and compare climate parameters with changed vegetation patterns. Among the recent effective methods, Machine Learning (ML) and time-series models, which incorporate environmental and climate factors like temperature and humidity, have proven valuable in enhancing prediction accuracy (Lemenkova, 2023c, 2024c; Asghar Rostami et al., 2025; Lee et al., 2025; Mucomole et al., 2025).

Recent research emphasizes various approaches to model and predict behaviour of climate and hydrological variables in forest ecosystems, exploring both statistical and ML models in diverse agricultural contexts (Lemenkova P., 2021c, 2021d, 2022b; Fu et al., 2024; Sharp et al., 2025; Ozdemir & Abdikan, 2025). To solve numerical equations of atmospheric physics and dynamics in forest ecosystems using ML tools, such atmospheric models need calculated variables on energy, moisture, and momentum fluxes at the land surface as boundary conditions. Building on previous findings that use advanced techniques (RS, DL, ML, and time-series models) to provide an integrated method for tracking and predicting connectivity between environmental variables (Lemenkova, 2022c, 2023b; Bilgilioğlu et al., 2024; Olarte et al., 2024), the methodology of this study combines statistical framework, optimized for real-time identification of effects of tree characteristics (age and height of canopy) on water balance in the coniferous forests of the Tyrolean Alps to predict hydro-environmental trends based on the observation data.

METHODS

Study area

In this study, we presented climate model simulations in temperate coniferous forests that show that Alpine forests maintain high rates of evapotranspiration, decrease surface air temperature, and increase precipitation rates. The experiment was conducted in South Tyrol, in the Italian Alps (1735 m a.s.l., 46°35′11″N, 11°26′00″E), Figure 1.

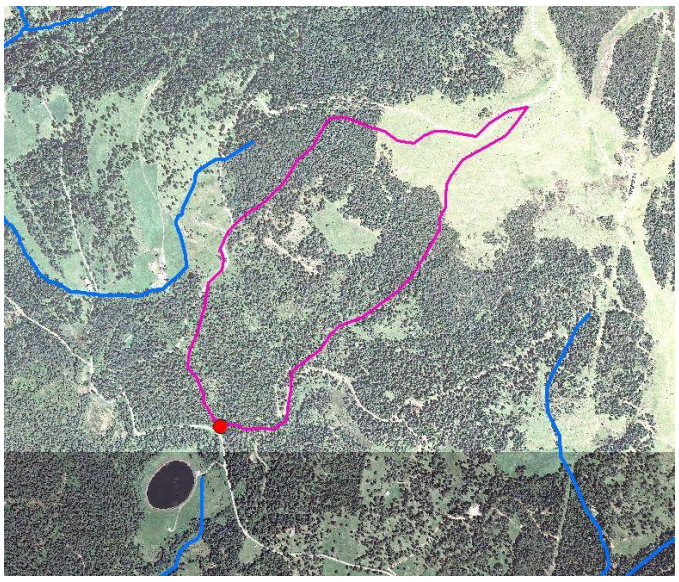

Figure 1. Aerial view of the study area.

The catchment has an area of 0.44 km^2. The water basin was measured on the local digital elevation model using ArcGIS software. The total of 85% spruce [*Picea abies (L) Karst.*], 12% Swiss stone pine (*Pinus cembra L.*), and 3% European larch (*Larix europea L.*) trees made up the tree layer (diameter at breast height (DBH) >5 cm). Individuals of European rowan (*Sorbus aucuparia*) and Scots pine (*Pinus sylvestris L.*) were also uncommon. About 29 meters was the height of the dominating tree. Alpenrose (*Rhododendron ferrugineum L.*) and blueberries (*Vaccinium myrtillus L.*) made up the majority of the understory. *Deschampsia flexuosa (L.)* Trin, or wavy hair-grass, predominated in the intervening grasslands.

Prediction of fog based on meteorological conditions during days with rain, fog and mixed precipitation

In order to understand the weather conditions throughout dry and wet circumstances, and particularly during the days with fog presence (visible below 1 km), meteorological variables measured between 2015 and 2019 were analyzed. The ratio of diffuse to total global radiation, the VPD, and relative air humidity (RH) were chosen to characterize hours and days without precipitation, with fog-only, with rain-only, and with mixed precipitation (fog and rain). The measurement was performed using equipment in Figure 2.

Figure 2. Pulvometers used in the study area: young forest (<30 years, left) and old forest (>200 years, right).

The climate benefits of forests because coniferous trees regulate temperature, control water balance and contribute to balanced albedo. In this regards, forests mitigate negative effects from climate change. Hence, afforestation decreases climate warming. Consequently, it is recommended to continue protection of forest stands in Alpine ecosystems and maintain precious coniferous stands. Such land use policies in Alps should consider the impacts of forest on climate, their effects on water balance at different spatial and temporal scales, and their effectiveness and sustainability as ecosystem service regulator.

The methodology of this study is based on the integrated assessment of climate parameters and the impacts from the young and old forest stands indicated on the cartographic plot, Figure 3. Specifically, this entails an evaluation of albedo, evapotranspiration (ET), transpiration (T), temperature and fog frequency. The evaluation of these parameters in young and old tree stands enables to assess non-linear complex relationships between forest vegetation and climate settings in the coniferous ecosystems of Alps. The geographic impact of these processes varies, because it depends on the time scale of climate forces. For instance, greenhouse gases are also well mixed in the atmosphere and influence global climate which can affect forest and regional impact of the biogeophysical feedbacks.

In turn, the biogeophysical processes influence climate as illustrated below on the models. These processes provided the expected throughfall for a certain precipitation event that included both fog (mixed precipitation) and rain alone. The difference between measured throughfall and the rain-to-throughfall contribution, which was determined by multiplying precipitation by the slope of the throughfall to precipitation equation from rain-only occurrences, was then used to estimate the fog contribution to throughfall for days with mixed precipitation. Using the existing methodology, the impact of fog on throughfall was used to assess its role and contribution. For mixed precipitation and rain-only events, we first calculated a linear regression equation between throughfall and precipitation rates for both stands.

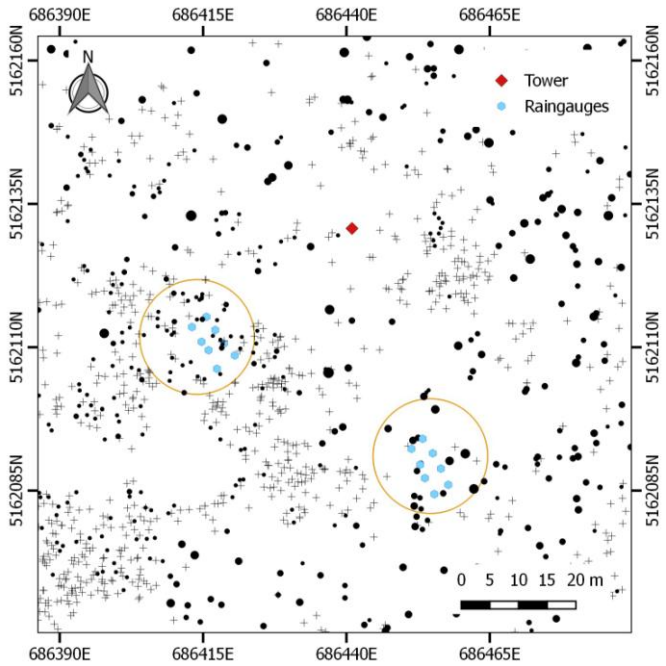

Figure 3. Map (100*100m) showing location of the inspected trees. Software: ArcGIS.

Calculation of Evapotranspiration

Evapotranspiration (ET_EC) was computed using Eddypro software and eddy covariance data in accordance with the ICOS setup. The systematic errors was calculated in the eddy covariance measurements for LE+H at the Renon site to be 17.6% based on the monthly energy balance ratio (EBR) data. It is reasonable to suppose that this mistake is half of the amount in LE (8.8%), and hence in ET, given a Bowen ratio of 1 in the summer. Figure 4 displays the additional elements of the water balance as well as the random error of EC.

Heat balance measurements

In addition to contributing to the terrestrial carbon sink, boreal ecosystems store a significant amount of carbon in soil, permafrost, and wetlands, and mature forests have a low yearly carbon gain. Five spruce trees with a DBH ranging from 23 cm to 57 cm had their sap flow measured in order to determine tree transpiration. Up to ten trees' sap flow measurements dating back to 2016 revealed that these trees behaved in a way that was typical of their size classes. One tissue heat balance sensor (Table 1) was placed at the north side of the trees to reduce mistakes caused by incoming shortwave radiation. Sap flow rates for the entire sapwood depth per unit trunk circumference (kg $^{h-1}$ cm^{-1}) were included into the measuring system. After logging the detected values at 10-minute intervals, we multiplied them by the stem circumference (less the thickness of the bark andphloem measured during sensor testing) to scale them to the tree level.

Computing sap flow

We compared the 95th percentile (P95) of 30-min sap flow rates for 2019 and the prior years to see if wound reactivity and/or resin buildup caused a drop in sap flow while a sensor remained in place for more than a year. We discovered that the P95 sap flow for the two smallest trees had significantly decreased. As a result, we multiplied the P95 [(year of sensor installation)/P95(2019)] ratio to get the rectified sap flow for 2019. A linear correlation between the sap flow of the corresponding tree and eddy covariance evapotranspiration (R2 = 0.57 to 0.66 at a 30-min resolution) was employed to fill up minor data gaps brought on by power outages or transient sensor malfunctions.

Days with precipitation (which we counted as days with mixed precipitation) were frequently accompanied by fog. During a monitoring period of 167 days (from late spring to autumn of 2019), there was fog for 241 hours during 9 days with fog (5%) and 45 days with mixed precipitation (27%).

Meteorological conditions and hydrological components

Flux energy measurements provided in this study confirm that coniferous forests have lower albedo for old forests compared with young forests, greater net radiation, and greater evapotranspiration, particularly during the summer season, producing a shallow, cool, and moist boundary layer. These findings emphasize how crucial are days with both fog and precipitation (mixed precipitation). No fog or mixed precipitation data were obtained during the 254 days of overcast conditions (70%) that were observed in South Tyrol in 2011. According to our 2019 data, 45% of overcast days in 2011 might have been fog days (defined as days with fog and mixed precipitation). For the entire observed time in 2015 and

2019, as well as the common period observed in both years, there were days with dry weather, fog and precipitation (rain or snowfall), and mixed precipitation of fog and rain or snowfall, Table 1.

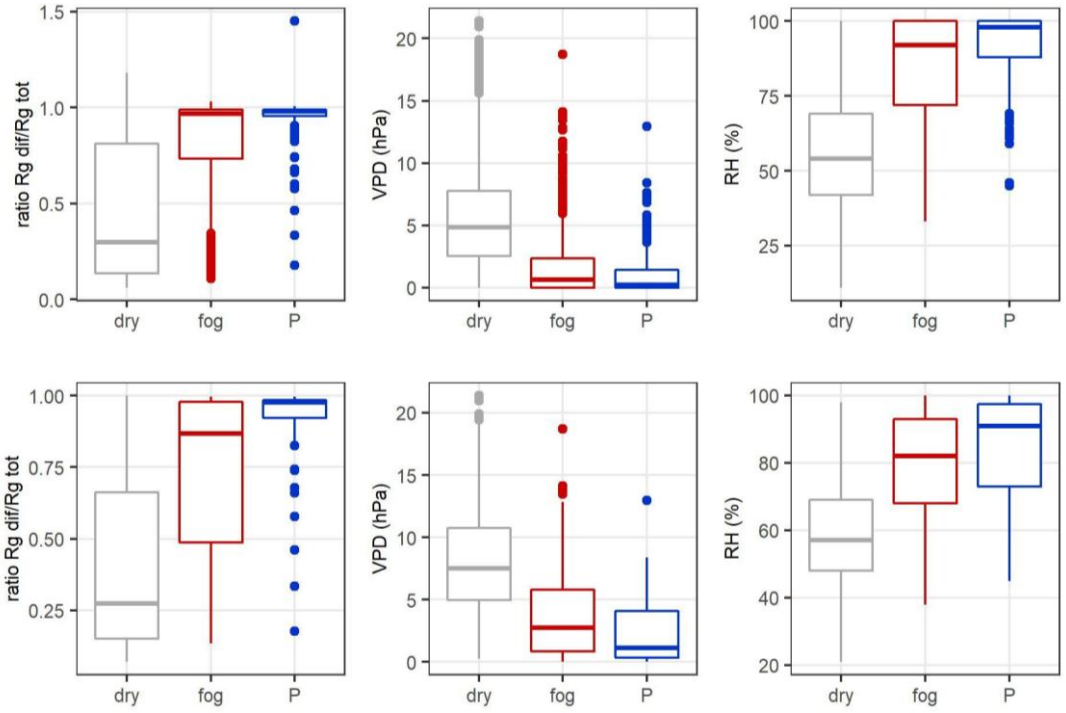

Figure 4. Weather conditions at times of fog (less than 1 km visibility), precipitation, and dry conditions (dry) from 01/01/2015 to 30/08/2015 (top row) and from 25/05/2015 to 30/08/2015 (bottom row) (ratio of diffuse to total global radiation, vapor pressure deficit VPD, and relative air humidity RH).

Table 1. Technical description and accuracy of the instrumentation used to calculate water balance.

Description	Height above	Nr. of sensors	Period of measurements	Instrument uncertainty	Instrument type
Evapotranspiration with Eddy covariance	33.7	1	Long term	±8.8%	Gill HS100 (Gill Instruments Inc.)
Gloval and diffuse radiation	40.3	1	Long term	±5%	DeltaT SPN1 (Delta Devices)
Net radiation	—	1	Long term	—	CNR4net radiometer
—	—	—	—	±0.5% rh	RM Young screen and
Relative humidity	33	1	Long term	—	—
Precipitation - open field	2	1	Long term	±3%	Geonor T200b (Geonor)
Fog frequence (visibility)	32	1	Jan 2015 - Dec 2015	N.A.	Netcam SC5
—	N.A.	1	Jan 2019 - Nov 2019	N.A.	—
Sap flow	DBH	5 spruce trees	Long term	±20% (1)	Tissue heat balance sensors
Temperature inside the canopy	15,23	2	Long term	0.1% at 25 C	Tinytag Data 2; Gemini Datalogger
Humidity inside the canopy	15,23	2	Long term	±3.0% RH at 25 C	Tinytag Data 2; Gemini Datalogger
Precipitation - below canopy, throughfall	0.3	16	Jun-Nov 2019	±1%	Stocker 4523
Precipitation - below canopy, throughfall	0.3	6	Jun-Nov 2019	±1%	Onset (S) RGX + Hobo logger
Precipitation - below canopy, stemflow	0.3	2	Jun-Nov 2020	±1%	Onset (S) RGX + Hobo logger
Soil water content	-0.05, -0.10, -0.20,				
Water discharge	0—2	1	One year (2019)	±0.1%	OTT CTD sensor

The measured values were logged at 10-min intervals and then scaled to the tree level by multiplying them with stem circumference (minus the bark and phloem thickness measured during sensor installation) and integrated them to 30-min and daily sums per tree (L day^{-1}), Table 2.

The systematic error was computed for I in Eq. 2 as well as the equipment accuracy of the measured variables. Given their excellent correlations ($R^2 > 0.87$), linear correlation with operational gauges was used to fill in data gaps caused by logger failure. The manual gauge data, which was absent for the most recent sampling interval, was added using a linear correlation with the automatic gauge results (R^2>0.77). The study site did not have direct access to long-term fog data. As a result, the information from the 2015 and 2019 was obtained.

Table 2. Meteorological parameters for varied weather conditions (dry and wet) according to the observations: measuring period, time observed and days.

Year	2015 all		2015 common period		2019 all		2019 common period	
period	1.1--30.8.2015		25.5--30.8.2015		25.5--7.11.2019		25.5--30.8.2019	
Time	9:00-17:00		9:00-17:00		0:00-24:00		0:00-24:00	
	days	%	days	%	days	%	days	%
Dry	123	50.6	40	41.2	79	47.3	46	47.4
Fog	72	29.6	31	32.0	9	5.4	2	2.1
rain/snow	11	4.5	6	6.2	34	20.4	31	32.0
mixed precipitation	37	15.2	20	20.6	45	26.9	18	18.6
Total	243	100	97	100	167	100	97	100

Overall, there were 296.5 hours of fog between January and August with 72 days of fog and 37 days of mixed precipitation (109 days; 30% of days were foggy and 15% had mixed precipitation). Days with fog were common in 2019, although there weren't many days with just fog.

RESULTS AND DISCUSSION

Long term precipitation and fog frequency

In this study, we demonstrated the deep links between the coniferous forests and climate throug hevaluated parameters of precipitation and fog frequency. Boreal forests are vulnerable to global warming. In the studied boreal forests of the Alps, there may be loss of evergreen trees and a shift toward deciduous trees due to the climate change. Increased disturbance from fire or insect outbreaks will shift the old coniferous forest to a younger ages. Climate forcing arising from younger stand age may be comparable to that arising from biome shifts. To forecast the incidence of fog in 2019, average radiation, relative humidity, and vapour pressure deficit (VPD) values for days with precipitation, fog, and mixed precipitation in 2015 were computed. When total Rg was high during dry periods, the ratio of total to global radiation (ratio Rg dif/Rg tot) was lower. Conversely, fog and rain had less of an impact on diffuse Rg. The relative air humidity (RH) was lower and VPD was higher during dry conditions than during fog and precipitation, as was to be expected. Compared to the RH and VPD, the Rg dif/Rg tot ratio had more data variability.

When examining time courses, it was found that air temperature (T) and VPD were often lower on foggy and wet days, increased on the first dry days, and then declined once again as the measuring period came to a conclusion. In contrast to T and VPD, relative humidity showed the opposite pattern. According to long-term statistics in Europe, fog caused the temperature to rise at night while decreasing during the day; this suggests that the temperature is more sensitive at night.

Tree transpiration and canopy evapotranspiration

The division of net radiation into sensible and latent heat fluxes varies among boreal forests. Compared to deciduous broadleaf forests, conifer forests produce higher rates of sensible heat exchange and deep atmospheric boundary layers because they have a lower midsummer evaporative fraction, which is the ratio of latent heat flow to accessible energy. Thus, with just one 5-day dry spell at the end of June and another 13 days in mid-September, rainfall events happened fairly often over the whole 2019 measuring period, despite the fact that the precipitation totals in June were lower than the long-term average (Figure 4).

Synthesis of flux data from boreal and temperate Alpiine regions in various stages of ecosystem development (old and young stands) is essential to understand the functioning of forests. It enables to better understand the variations of climate responses across gradients of climate, soils, land cover types, and plant functional patterns. Hence, time courses of T and ET showed good correspondence with similar responses to weather conditions and an overall decrease beginning in late September, but the transpiration of the old (Tof) and young stand (Tyf), as determined by sap flow measurements, was low in comparison to canopy evapotranspiration from eddy covariance, which applied to both stands. The Tyf was higher than Tof as the new stand's higher tree density and smaller projected crown area more than made up for the old stand's larger sap flow from massive single trees. As a result, for both forest types, the Tyf to ET regression line sloped higher than the Tof to ET one. The association between T and ET had an R2 value greater than 0.9. On the other hand, there was no correlation between P and ET or T.

Flux measurements illustrate the potential for changes in species composition, arising from change in the climate regime, to affect water cycle in forests. For example, we found that ET was higher on dry days (55% of total ET in 48% of days) and suppressed, particularly on days with mixed precipitation (17% of total ET in 26% of days), when we divided the days into dry, mixed precipitation (fog and precipitation), and rainfall-only (Table 2). This is due to fog lowering ET, as seen in cloud forests, and also because mixed precipitation days were more frequent in autumn, when ET was normally lower due to phenology (senesced grasses) and lower temperatures.

Although the LAI in both stands was identical, the new stand had higher throughfall rates in relation to precipitation than the old stand. Because the manual gauges covered a larger small-scale fluctuation of PAI/LAI, their throughfall variability was higher than that of the automatic ones. A strong linear correlation ($R^2 > 0.93$) was found between throughfall and precipitation for both stands and no clear increase in throughfall ratio with P. The last data point with the highest amount of throughfall and P was clearly above the linear regression line, indicating that the limits of the canopy's interception capacity were reached. The correlation between old and young forest stand throughfall is very high.

The same water components, divided into roughly monthly intervals (adjusted to the manual throughfall gauges' sampling periods), show that P rose from June to October and ET peaked in September before sharply declining after that. Except for June in the old stand, the Tf/P ratio was higher in the fall (September and October) than in the summer, and as a result, the interception rate (I/P) was lower.

Throughfall rates were much greater on days with mixed fog and rain precipitation, whereas interception rates (I/P) were lower on days with rain only. This was discovered by examining throughfall rates at a daily resolution and differentiating by precipitation type. Fog was blamed for this Tf excess (Tf/P = 0.28 for the young stand and Tf/P = 0.27 for the old stand). In addition to having more mixed precipitation days in the fall, this should be linked to greater P. Furthermore, stemflow, which was comparable for both stands, rose between June and October but was still too low overall to significantly affect the water balance. Variations in height and air temperature could account for the Alpine forest's reduced contribution. This finding supports our theory that fog may very slightly affect the seasonal and annual water budget.

Water partitioning and balance at catchment level

Over the course of the 5-month measurement period, we noticed a number of variations in the ecosystem water partitioning between the young and old forest (Table 3).

Table 3. Meteorological parameters for forest with young and old stands. Water components at canopy level for five months, from 2019-5-30 (DOY 150) to 2019-11-07, are approximately separated into months based on the manual throughfall gauges' sampling dates.

Days with mixed precipitation	young forest	old forest
P measured (mm)	460 ± 35	460 ± 35
Total Tf measured (mm)	292 ± 26	216 ± 11
Tf from rain only events (mm)	243 ± 7	184 ± 8
Fog in mixed events (mm)	70 ± 15	53 ± 5
measured Tf/P (%)	64	47
estimated rain-only Tf/P (%)	53	40
estimated fog Tf/P (%)	15	12
rain contribution to Tf (%)	83	84
fog contribution to Tf (%)	24	24

The young forest had higher levels of transpiration and throughfall. As a result, the young stand had reduced interception, which was determined by subtracting Tf from Sf and then subtracting total P. Interception was responsible for a significant portion of ET (54% in the ancient forest and 33% in the young forest), as intercepted water eventually evaporates back to the sky. Rainfall water can return to the atmosphere more quickly by evaporation, which is a component of the water cycle, rather than via the soil or plant life. When compared to other conifer forests studied in the literature, where T/ET, T/P, and T/potential ET ratios range from 15% to 75%, the ratios of transpiration measured with sap flow to evapotranspiration from eddy covariance (T/ET = 22% for of, 31% for yf) or total precipitation (T/P = 24% for of, 34% for yf) were low for both stands. However, in contrast to I/P reported values of 17–45%, our high ratios of interception to precipitation (I/P = 54% for of, 33% for yf) and ET (I/ET = 51% for of, 31% for yf) were in the upper range.

CONCLUSION

Much of our understanding of how forest impacts climate, and our ability to mitigate climate change, comes from simulation and modelling techniques. Models of climate and the forest biosphere are simplifications of complex physical, chemical, and biological processes in the boreal forest ecosystems. Using such modelling techniques, this study shows that forest age and height are potential climate regulators in the coniferous forests.

Extrapolation of process-level functioning of forest ecosystem functioning was gained from modelling experiments and field studies. Here, the biosphere models were constrained with observational data across a scale from in situ measurements, flux heat computations of ecosystem functioning and syntheses of ecosystem research. The low transpiration/ET ratios can be explained by modelled link between forest ecosystems and climate parameters. Calculated as the residual of ET (Eddy covariance) - T - I, the evapotranspiration of the soil and understory was higher in the young stand, where the interception was significantly lower. Additional information might be obtained by an independent measurement of soil/understory ET utilizing canopy chambers or small-scale lysimeters. The water balance was completed by discharge (DC) and change in soil moisture (dSWC); since both were only measured for the entire forest, the same values were applied to both types of forests. Compared to T and Esu, DC and dSWC were both insignificant. Before the measuring period began, the majority of the discharge happened during the spring snowmelt. Only on short time scales do changes in soil moisture matter when calculating the water balance, and they have essentially leveled out during measurement period.

The temperate coniferous forests in the Alps are linked with climate forces. The biogeophysical parameters such as low albedo during winter and ET during summer influence annual mean T. Higher albedo with loss of forest cover could offset carbon emission so that the net climatic effect of temperate deforestation is negligible, or reduced ET with loss of trees could amplify biogeochemical warming. Although the amount of water input from fog only events at our site was unknown, fog was projected to contribute 24% more throughfall than rain-only events, indicating a clear contribution to mixed fog and rain precipitation. Importantly, previous studies did not take fog into account. Therefore, fog is the missing link in our current findings to comprehend both the decrease of evaporative conditions during dry periods in the studied Alpine environment and the recharge of soil water during days with mixed precipitation.

The ability of the intercepted water to function as a climate regulator at the local and mesoscale is climatologically significant, in addition to the physiological element of the plant's water use. By emitting 44.2 W m^{-2} of latent heat instead of sensible heat, one millimeter of water at 20 °C lowers the temperature and increases the amount of water vapor in the atmosphere.

REFERENCES

Asghar Rostami, A., Taghi Sattari, M., Apaydin, H. & Milewski, A. 2025. Modeling Flood Susceptibility Utilizing Advanced Ensemble Machine Learning Techniques in the Marand Plain. Geosciences, 15, 110. https://doi.org/10.3390/geosciences15030110

Ahmed, A., Rotich, B. & Czimber, K. 2025. Climate Change as a Double-Edged Sword: Exploring the Potential of Environmental Recovery to Foster Stability in Darfur, Sudan. Climate, 13, 63. https://doi.org/10.3390/cli13030063

Bilgilioğlu, S. S., Gezgin, C., Iban, M. C., Bilgilioğlu, H., Gündüz, H. I. & Arslan, Ş. 2025. Explainable Sinkhole Susceptibility Mapping Using Machine-Learning-Based SHAP: Quantifying and Comparing the Effects of Contributing Factors in Konya, Türkiye. Appl. Sci, 15, 3139. https://doi.org/10.3390/app15063139

Cai, Y. & Shi, X. 2025. A Comparative Study on the Methods of Predictor Extraction from Global Sea Surface Temperature Fields for Statistical Climate Forecast System. Atmosphere, 16, 349. https://doi.org/10.3390/atmos16030349

Can, M., Vaheddoost, B. & Safari, M. J. S. 2025. Data Reconstruction for Groundwater Wells Proximal to Lakes: A Quantitative Assessment for Hydrological Data Imputation. Water, 17(5), 718. https://doi.org/10.3390/w17050718

Crișu, L., Zamfir, A.-G., Vlăduț, A., Boengiu, S., Simulescu, D. & Mititelu-Ionuș, O. 2025. Assessing Vegetation Response to Drought in the Central Part of Oltenia Plain (Romania) Using Vegetation and Drought Indices. Sustainability, 17, 2618. https://doi.org/10.3390/su17062618

Fu, Y., Tan, H., Kou, W., Xu, W., Wang, H. & Lu, N. 2024. Estimation of Rubber Plantation Biomass Based on Variable Optimization from Sentinel-2 Remote Sensing Imagery. Forests, 15, 900. https://doi.org/10.3390/f15060900

Ji, P., Su, R., Wu, G., Xue, L., Zhang, Z., Fang, H., Gao, R., Zhang, W. & Zhang, D. 2025. Projecting Future Wetland Dynamics Under Climate Change and Land Use Pressure: A Machine Learning Approach Using Remote Sensing and Markov Chain Modeling. Remote Sens., 17, 1089. https://doi.org/10.3390/rs17061089

Kang, M., Cho, S., Kim, S. J., Kim, E. & Kang, M. 2025. Deviations in evapotranspiration measurements between enclosed- and open-path eddy covariance systems. Hydrological Sciences Journal, pp. 1-9. https://doi.org/10.1080/02626667.2025.2463619

Klaučo, M., Gregorová, B., Stankov, U., Marković, V. & Lemenkova, P. 2013. Determination of ecological significance based on geostatistical assessment: a case study from the Slovak Natura 2000 protected area. Central European Journal of Geography. 5, pp. 28-42. https://doi.org/10.2478/s13533-012-0120-0

Lee, J., Han, J., Engel, B. & Lim, K. J. 2025. Web-Based Baseflow Estimation in SWAT Considering Spatiotemporal Recession Characteristics Using Machine Learning. Environments, 12, 94. https://doi.org/10.3390/environments12030094

Lemenkova, P. 2021a. Evaluating land cover types from Landsat TM using SAGA GIS for vegetation mapping based on ISODATA and K-means clustering. Acta agriculturae Serbica, 26(52), pp. 159-165. https://doi.org/10.5937/AASer2152159L

Lemenkova, P. 2021b. Mapping environmental and climate variations by GMT: A case of Zambia, Central Africa. Zemljište i biljka, 70(1), pp. 117-136. https://doi.org/10.5937/ZemBilj2101117L

Lemenkova, P. 2021c. ISO Cluster classifier by ArcGIS for unsupervised classification of the Landsat TM image of Reykjavík. Bulletin of Natural Sciences Research, 11(1), pp. 29-37. https://doi.org/10.5937/bnsr11-30488

Lemenkova, P. 2021d. Distance-based vegetation indices computed by SAGA GIS: A comparison of the perpendicular and transformed soil adjusted approaches for the LANDSAT TM image. Poljoprivredna tehnika, 46(3), pp. 49-60. https://doi.org/10.5937/PoljTeh2103049L

Lemenkova, P. 2022a. Evapotranspiration, vapour pressure and climatic water deficit in Ethiopia mapped using GMT and TerraClimate dataset. Journal of Water and Land Development, 54(7-9), pp. 201-209. https://doi.org/10.24425/jwld.2022.141573

Lemenkova P. 2022b, Mapping Ghana by GMT and R scripting: advanced cartographic approaches to visualize correlations between the topography, climate and environmental setting, Advances in Geodesy and Geoinformation, 71, 1, e16. https://doi.org/10.24425/gac.2022.141169

Lemenkova, P. 2022c. GRASS GIS Scripts for Satellite Image Analysis by Raster Calculations Using Modules r.mapcalc, d.rgb, r.slope.aspect. Tehnički vjesnik, 29, 6, pp. 1956-1963. https://doi.org/10.17559/TV-20220322091846

Lemenkova P. 2023a. Monitoring Seasonal Fluctuations in Saline Lakes of Tunisia Using Earth Observation Data Processed by GRASS GIS, Land, 12, 11, 1995. https://doi.org/10.3390/land12111995

Lemenkova, P. 2023b. Mapping Wetlands of Kenya Using Geographic Resources Analysis Support System (GRASS GIS) with Remote Sensing Data. Transylvanian Review of Systematical and Ecological Research, 25, 2, pp. 1-18. https://doi.org/10.2478/trser-2023-0008

Lemenkova P. 2023c. A GRASS GIS Scripting Framework for Monitoring Changes in the Ephemeral Salt Lakes of Chotts Melrhir and Merouane, Algeria. Applied System Innovation, 6, 4, 61.

Lemenkova, P. 2024a. Artificial Intelligence for Computational Remote Sensing: Quantifying Patterns of Land Cover Types around Cheetham Wetlands, Port Phillip Bay, Australia. Journal of Marine Science and Engineering, 12, 8, 1279. https://doi.org/10.3390/jmse12081279

Lemenkova, P. 2024b. Support Vector Machine Algorithm for Mapping Land Cover Dynamics in Senegal, West Africa, Using Earth Observation Data. Earth, 5, pp. 420-462. https://doi.org/10.3390/earth5030024

Lemenkova, P. 2024c. Machine learning methods of satellite image analysis for mapping geologic landforms in Niger: A comparison of the Aïr mountains, Niger River basin and Djado Plateau. Podzemni radovi, 45, pp. 27-47. https://doi.org/10.5937/podrad2445027L

Lindh, P. & Lemenkova, P. 2023. Effects of Water—Binder Ratio on Strength and Seismic Behavior of Stabilized Soil from Kongshavn, Port of Oslo. Sustainability, 15(15), 12016. https://doi.org/10.3390/su151512016

Minić, V. 2001. Hydrogeological influence of the Rautovac stream basin upon the quality of the Niška Banja thermal waters. Acta medica Medianae, 40(4), pp. 5-37.

Mucomole, F. V., Silva, C. A. S. & Magaia, L. L. 2025. Experimental Parametric Forecast of Solar Energy over Time: Sample Data Descriptor. Data, 10, 37. https://doi.org/10.3390/data10030037

Olarte, E., Gutierrez, J., Roque, G., Soria, J. J., Fernandez, H., Carpio, J. E. P. & Poma, O. 2025. Predictive Model with Machine Learning for Environmental Variables and PM2.5 in Huachac, Junín, Perú. Atmosphere, 16, 323. https://doi.org/10.3390/atmos16030323

Ozdemir, E. G. & Abdikan, S. 2025. Forest Aboveground Biomass Estimation in Küre Mountains National Park Using Multifrequency SAR and Multispectral Optical Data with Machine-Learning Regression Models. Remote Sens., 17, 1063. https://doi.org/10.3390/rs17061063

Ristić Vakanjac, V., Nikić, Z., Vakanjac, B. & Rašić, D. 2015. Analysis of the regime and water balance Dojkinacka river. Pirotski zbornik, 40, pp. 183-201. https://doi.org/10.5937/pirotzbor1540183R

Roljević, S., Nikolić, A. & Tepavac, R. 2012. The consumption of mineral fertilizers and water resources' quality in the European Union and the Republic of Serbia. Ekonomika poljoprivrede, 59(1), pp. 139-146. https://www.ea.bg.ac.rs/index.php/EA/article/view/601

Shaddad, S., Castrignanò, A., Di Curzio, D., Rusi, S., Abu Salem, H. S. & Nosair, A. M. 2025. An Integrated Statistical, Geostatistical and Hydrogeological Approach for Assessing and Modelling Groundwater Salinity and Quality in Nile Delta Aquifer. Agri Engineering 7, 34. https://doi.org/10.3390/agriengineering7020034

Sharp, K. G., Bell, J. R., Pankratz, H. G., Schultz, L. A., Lucey, R. Meyer, F. J. & Molthan, A. L. 2025. Modifying NISAR's Cropland Area Algorithm to Map Cropland Extent Globally. Remote Sens., 17, 1094. https://doi.org/10.3390/rs17061094

Zhang X., Liu Y., Chen R., Si M., Zhang C., Tian Y. & Shang G. 2025. The Spatiotemporal Evolution and Driving Forces of the Urban Heat Island in Shijiazhuang. Remote Sensing, 17(5), 781. https://doi.org/10.3390/rs17050781

Zhu, S., Quaife, T. & Hill, T. 2024. Uniform upscaling techniques for eddy covariance FLUXes (UFLUX). International Journal of Remote Sensing, 45(5), pp. 1450-1476. https://doi.org/10.1080/01431161.2024.2312266